Quantum Diffusion in Liquid Para-hydrogen: An Application of the Feynman−Kleinert Linearized Path Integral Approximation†

Jens Aage Poulsen and Gunnar Nyman

Physical Chemistry, Gøteborg University, S-412-96, Göteborg, Sweden

Peter J. Rossky*

Institute for Theoretical Chemistry, Department of Chemistry and Biochemistry, University of Texas at Austin, Austin, Texas 78712

Received: June 10, 2004; In Final Form: October 14, 2004

Quantum effects on diffusion in liquid para-hydrogen at temperatures of $T = 17$ and 25 K and saturated vapor pressure is studied by calculating the diffusion coefficient from the standard Green−Kubo formula, using both the ordinary velocity correlation function (CF) and its Kubo-transformed counterpart. All CFs are calculated with a recently proposed linearized path integral expression for general CFs, using an approximate Wigner transformed Boltzmann operator based on Feynman−Kleinert variational path integral theory. Also, the ability of the approximate Wigner transform to predict the radial distribution function and kinetic energy of the liquid is investigated. The conclusions are as follows: (i) The predicted structure of liquid para-hydrogen is in excellent agreement with accurate path integral Monte Carlo calculations at both temperatures. (ii) The calculated liquid kinetic energy is in very good agreement with the accurate value at $T = 25$ K but deviates somewhat from the accurate value at $T = 17$ K. (iii) The diffusion coefficients based on the Kubo-transformed CF are in very good agreement with experiment, at both temperatures, whereas results from the ordinary velocity CF are not accurate at $T = 17$ K. The reason for the better performance of the Kubo CF approach is attributed to the latter's robustness toward errors in the approximate Boltzmann operator Wigner transform. The kinetic energy derived from the Kubo-transformed CFs is in excellent agreement with accurate values at both temperatures.

1. Introduction

During the past decade, practical and general methods for calculating liquid-state correlation functions have been developed. Among these, we find the forward−backward semiclassical scheme,[34,53] the centroid molecular dynamics (CMD) algorithm,[5,21,22] and a recent implementation of the linearized path integral (LPI) representation of CFs, using a specific Feynman−Kleinert (FK) version of the Boltzmann Wigner transform (hence termed FK−LPI).[36] These methods represent practical schemes that strive for a compromise between the two, apparently incompatible, extremes: a method capable of accurately describing the quantum dynamics of large systems *and* a computational feasibility comparable to that of classical molecular dynamics codes. The aforementioned methods achieve this compromise by sacrificing the description of long-time coherence effects and, instead, focusing only on short-time interference phenomena. The daunting problem of propagating dynamics quantum-mechanically is bypassed by this focus, while retaining quantum mechanical probability distributions. The quantum statistical many-body dynamics then becomes computationally accessible. Therefore, it has been possible to apply these methods to dynamical phenomena in liquids where comparisons between theory and experiment are possible. The liquid-state applications of CMD,[3,20] forward−backward semiclassical dynamics,[34,53] maximum entropy analytical continuation schemes,[25−27,39,48] and the classical Wigner/LPI method[37,44,45] have demonstrated an acceptable level of accuracy and computational practicality of these methods, and that the accurate treatment of only short-time interference effects indeed does not seem to present a basic limitation.

The neglect of long-time interference effects is an approximation that works well in condensed phases. It is worth elaborating on this point. There has been much work devoted to the study of the quenching of interference effects when a "system" couples to a dissipative "bath", the latter mostly modeled as a set of harmonic oscillators (see, e.g., refs 2, 14, and 17). The essence of these studies is that the system-reduced density matrix rapidly becomes diagonal when the system and bath are allowed to interact. This effect, which is known as decoherence,[17] can be shown by a path integral analysis to generate classical and noise-free dynamical behavior for the system degree of freedom, augmented with a Wigner distribution for its initial phase-space distribution, *if* the system possess a sufficient inertia (see section VI.B. of ref 14).

The classical Wigner/LPI model can be derived by a related analysis, which is also justified when decoherence is strong.[36] The chain of reasoning is as follows. One starts from the exact path integral (PI) expression for the desired system CF. First, it is noted, as is also well-known,[14] that forward−backward system paths must inherently be similar to make any significant contribution to the CF value. This occurs because of the assumption of strong system−bath coupling. As a consequence, the PI action functional may be linearized in the system degree

† Part of the special issue "Frank H. Stillinger Festschrift".

* Author to whom correspondence should be addressed. Telephone: 512-471-3555. Fax: 512-471-1624. E-mail address: rossky@mail.utexas.edu.

10.1021/jp040425y CCC: $27.50
Published on Web 11/16/2004

of freedom. Since each degree of freedom of the bath can be successively viewed as the "system", one may introduce the approximation of also linearizing that part of the PI action functional of each bath degree of freedom. As was recently shown,[36,46] this full linearization of the PI, termed LPI, yields the classical Wigner method or equivalently, the linearized semiclassical initial value representation (LSC−IVR) of CFs.[32] The analysis just given is important, because it shows not only how to derive the LPI method but also suggests under what conditions the LPI theory is expected to work. In passing, we note that Miller and co-workers,[32,50] Zhang and Pollak,[55] and Liao and Pollak[30] considered the accuracy of the classical Wigner/LPI method in different model problems. They explicitly demonstrated the accuracy of the LPI method for system−bath problems.

From the aforementioned discussion, it follows that the LPI approach to CFs is expected to perform best in the condensed phase, because of bath-induced decoherence. However, because of the challenging implementation of the Boltzmann Wigner transform, which contains a sign problem,[29] the LPI method has only very recently been applied to two realistic condensed-phase problems: the calculation of the spectrum of density fluctuations in liquid He(4), at 27 K,[37] and in the study of the vibrational relaxation of oxygen in liquid oxygen at 70 K.[44,45] In both of theses applications, LPI performed very well. In this paper, we report a new application of the LPI methodology, by applying the specific FK−LPI implementation of ref 36 to the problem of self-diffusion and structure in liquid para-hydrogen at almost zero pressure and temperatures of $T = 17$ and 25 K. The liquid model consists of 125 para-hydrogen molecules in a cubic box with periodic boundary conditions.

The purpose of this paper is 2-fold. The primary goal is the assessment of the accuracy of the LPI methodology for the diffusion problem. The second goal is to gain knowledge of the accuracy of the quantum statistics derived from the variational effective frequency theory of Giachetti and Tognetti[15,16] and Feynman and Kleinert.[13] The latter aim can be achieved by comparing radial distribution functions and kinetic energies from the variational theory with similar results obtained from accurate path integral Monte Carlo (PIMC) calculations.

The quantum diffusion in liquid para-hydrogen has been studied using several other methods, such as quantum mode coupling theory,[41] analytical continuation methods based on maximum entropy inversion,[40] forward−backward semiclassical dynamics,[34] CMD,[3,23,35,54] and path integral second moment Wigner semiclassical dynamics.[4] The predictions of FK−LPI can then readily be compared to other theoretical methods to evaluate its relative accuracy.

This paper is structured as follows. In section 2, the general LPI equations and the effective frequency representation of the Boltzmann operator are presented. In section 3, we develop the FK−LPI equations needed for calculating diffusion coefficients. In section 4, the details of the molecular dynamics (MD) simulation are addressed. In section 5, we present the numerical results. We finally conclude in section 6.

2. Theory

In the following subsections, we discuss each of the theoretical components required for the present application. We start by outlining the basics behind the LPI theory. We then present the effective frequency implementation of the Boltzmann operator, which allows for its analytical Wigner transform.

2.1. The Classical Wigner or Linearized Path Integral (LPI) Method. The subject of this paper concerns the application and implementation of probably the simplest approach to the dynamics of large quantum systems, namely, the so-called classical Wigner model or, equivalently, the linearized semiclassical initial value representation (LSC−IVR) of CFs.[18,19,36,43,51] It may be summarized as follows. To obtain the canonical CF $\langle \hat{A}(0)\hat{B}(t)\rangle$, one makes use of the approximate classical Wigner expression:

$$\langle \hat{A}(0)\hat{B}(t)\rangle \approx \frac{1}{(2\pi\hbar)^{3N}}\left(\frac{1}{Z}\right)\int\int \mathrm{d}\vec{q}\ \mathrm{d}\vec{p}\ (\exp(-\beta\hat{H})\hat{A})_{\mathrm{W}}[\vec{q},\vec{p}](\hat{B})_{\mathrm{W}}[\vec{q}_t,\vec{p}_t] \quad (1)$$

The interpretation of eq 1 proceeds as follows. Phase-space points $(\vec{q},\vec{p})$ are sampled from the Wigner transform of $\exp(-\beta\hat{H})\hat{A}$, the transform being defined for an arbitrary operator $\hat{C}$ by[52]

$$(\hat{C})_{\mathrm{W}}[\vec{x},\vec{p}] \equiv \int \mathrm{d}\vec{\eta}\ \exp(-i\vec{p}\cdot\vec{\eta}/\hbar)\left\langle \vec{x}+\frac{1}{2}\vec{\eta}\right|\hat{C}\left|\vec{x}-\frac{1}{2}\vec{\eta}\right\rangle \quad (2)$$

$(\vec{q},\vec{p})$ are evolved classically to $(\vec{q}_t,\vec{p}_t)$, which serves as the phase-space arguments of $(\hat{B})_{\mathrm{W}}[\vec{q}_t,\vec{p}_t]$. The term $3N$ represents the dimensionality of the problem. The expression in eq 1 follows from a path linearization approximation implemented within the semiclassical initial value representation (SC−IVR) of the propagator[19,51] or can be shown to follow quite directly from the exact quantum expression for the correlation function expressed in terms of Wigner phase space distributions, if the dynamical propagation is taken to be classical.[43] It has also been shown recently that the result follows from a path linearization approximation in the exact path integral expression for the CF, without the intermediate step of an SC−IVR formulation.[36,46] Hence, we have chosen a more descriptive phrase to refer to the approximation, namely the "linearized path integral" (or LPI) method. As opposed to forward−backward schemes,[34] the classical Wigner method is free of Herman−Kluk coherent state parameters that must be optimized. Notice that the LPI CF expression in eq 1 is equivalent to its classical counterpart, except through the usage of the Wigner-transformed operators. In the following, the three expressions "classical Wigner", LSC−IVR, and the LPI representation of CFs all refer to the identical approximation embodied in eq 1.

Before closing this section, we notice that the LPI approximation can be stated briefly in an alternative form. For $\hat{C}$ and $\hat{D}$ general operators:

$$\mathrm{Tr}\{\hat{C}\hat{D}(t)\} = \frac{1}{(2\pi\hbar)^{3N}}\int\int \mathrm{d}\vec{q}\ \mathrm{d}\vec{p}(\hat{C})_{\mathrm{W}}[\vec{q},\vec{p}](\hat{D}(t))_{\mathrm{W}}[\vec{q},\vec{p}] \approx \frac{1}{(2\pi\hbar)^{3N}}\int\int \mathrm{d}\vec{q}\ \mathrm{d}\vec{p}(\hat{C})_{\mathrm{W}}[\vec{q},\vec{p}](\hat{D})_{\mathrm{W}}[\vec{q}_t,\vec{p}_t] \quad (3)$$

Here, the Wigner-transformed Heisenberg operator, $(\hat{D}(t))_{\mathrm{W}}[\vec{q},\vec{p}]$, has been approximated by collecting all time dependence in the classical propagation of the phase-space arguments $(\vec{q}_t,\vec{p}_t)$.

2.2. The Feynman−Kleinert Linearized Path Integral Implementation. Recently, we suggested a route to the Wigner transform of the $\exp(-\beta\hat{H})\hat{A}$ operator, as required for LPI.[36,37] This approach was based on combining the effective frequency variational theory of Feynman and Kleinert (FK)[13] and Giachetti and Tognetti[16] with the quasi-density operator formalism of Jang and Voth.[21,58] The resulting CF approach, which is called FK−LPI, can be summarized as follows.

We consider a one-dimensional case. In one dimension, one may approximate the Boltzmann operator by

$$\exp(-\beta\hat{H}) \approx \int\int \mathrm{d}x_c\, \mathrm{d}p_c \rho_{FK}(x_c, p_c)\hat{\delta}_{FK}(x_c, p_c) \qquad (4)$$

where $\rho_{FK}(x_c, p_c)$ is the FK approximation to the centroid density:

$$\rho_{FK}(x_c, p_c) = \frac{1}{2\pi\hbar}\exp\left(-\beta\frac{p_c^2}{M}\right)\exp(-\beta W_1(x_c)) \qquad (5)$$

and $W_1(x_c)$ is the corresponding FK approximation to the centroid potential. The operator $\hat{\delta}_{FK}(x_c, p_c)$ is the effective frequency quasi-density operator:

$$\hat{\delta}_{FK}(x_c, p_c) = \int\int \mathrm{d}x\, \mathrm{d}x' \sqrt{\frac{M\Omega(x_c)}{\pi\hbar\alpha}}|x'\rangle\langle x| \times \exp\left[\frac{p_c}{i\hbar}(x'-x) - \frac{M\Omega(x_c)}{\hbar\alpha}\left(\frac{x+x'}{2} - x_c\right)^2 - \frac{M\Omega(x_c)\alpha}{4\hbar}(x'-x)^2\right] \qquad (6)$$

where α is a function of the effective frequency, $\Omega(x_c)$, through

$$\alpha = \coth\left(\frac{\Omega(x_c)\hbar\beta}{2}\right) - \frac{2}{\Omega(x_c)\hbar\beta} \qquad (7)$$

Performing a Wigner transform of eq 4 amounts to transforming $\hat{\delta}_{FK}$ (eq 6), which can be done analytically:

$$(\hat{\delta}_{FK}(x_c, p_c))_W[q, p] = \frac{2}{\alpha}\exp\left[-\frac{M\Omega(x_c)}{\hbar\alpha}(q-x_c)^2 - \frac{1}{M\Omega(x_c)\alpha\hbar}(p-p_c)^2\right] \qquad (8)$$

If $\hat{A}$ is a simple operator, the transform of $\exp(-\beta\hat{H})\hat{A}$ can also be obtained. For details, we refer the reader to ref 36. In section 3, it will be useful to express $\hat{\delta}_{FK}$ in a basis of momentum eigenstates, the latter expression which may be deduced from eq 6:

$$\hat{\delta}_{FK}(x_c, p_c) = \int\int \mathrm{d}p\, \mathrm{d}p' \sqrt{\frac{1}{\pi\hbar\alpha M\Omega(x_c)}}|p\rangle\langle p'| \times \exp\left[i\left(\frac{x_c}{\hbar}\right)(p'-p) - \frac{1}{\hbar\alpha M\Omega(x_c)}\left(\frac{p+p'}{2} - p_c\right)^2 - \frac{\alpha}{4\hbar M\Omega(x_c)}(p'-p)^2\right] \qquad (9)$$

Insertion of eq 8 into the Wigner transform of eq 4, followed by an integration over p_c, yields the alternative formula (cf. eq 48 in ref 36):

$$(\exp(-\beta\hat{H}))_W[q, p] = \int\frac{\mathrm{d}x_c}{2\pi\hbar}\rho_{FK}(x_c) \times \frac{2}{\alpha}\sqrt{\frac{M\alpha\pi}{(\beta/2)\coth(\hbar\Omega(x_c)\beta/2)}} \times \exp\left(-\frac{M\Omega(x_c)}{\hbar\alpha}(q-x_c)^2 - \left[\frac{\tanh(\hbar\Omega(x_c)\beta/2)}{M\Omega(x_c)\hbar}\right]p^2\right) \qquad (10)$$

where $\rho_{FK}(x_c) = \exp(-\beta W_1(x_c))$. The latter quantity allows for a classical-like calculation of the quantum partition function:[24]

$$Z_{FK} = \int \mathrm{d}x_c \sqrt{\frac{M}{2\beta\hbar^2\pi}}\rho_{FK}(x_c) \qquad (11)$$

The useful quantity of dimensional length squared,

$$a^2(x_c) \equiv \frac{\hbar\alpha}{2M\Omega(x_c)} \qquad (12)$$

is called the smearing width and measures the size of the particle position uncertainty when it is "centered" at x_c.[59] In many dimensions, the effective frequency representation of path integrals, independently proposed by Giachetti and Tognetti[15,16] and Feynman and Kleinert,[13] requires the effective frequencies, their associated effective frequency normal modes, and finally the centroid potential. A description of how these quantities are obtained can be found in refs 6, 9, and 36.

3. FK−LPI Equations for Green−Kubo Velocity CF Formula

We shall start with the derivation of the FK−LPI versions of the two formerly identical Green−Kubo expressions for the molecular center-of-mass diffusion constant:

$$D = \frac{1}{3N_{H_2}}\int_0^\infty \langle\vec{v}(0)\cdot\vec{v}(s)\rangle\, \mathrm{d}s \qquad (13)$$

and

$$D = \frac{1}{3N_{H_2}}\int_0^\infty \langle\vec{v}(0)\cdot\vec{v}(s)\rangle_K\, \mathrm{d}s \qquad (14)$$

where $\vec{v}$ denotes the $3N_{H_2}$ dimensional velocity vector of the N_{H_2} H_2 center-of-mass coordinates. $\langle\vec{v}(0)\cdot\vec{v}(s)\rangle$ and $\langle\vec{v}(0)\cdot\vec{v}(s)\rangle_K$ denotes the normal and Kubo-transformed velocity CF, respectively. The Kubo-transformed velocity CF is defined by[28,56]

$$\langle\vec{v}(0)\cdot\vec{v}(s)\rangle_K \equiv \frac{1}{\beta\hbar}\int_0^{\beta\hbar}\langle\vec{v}(-i\lambda)\cdot\vec{v}(s)\rangle\, \mathrm{d}\lambda \qquad (15)$$

As we shall explicitly see below, this folding is numerically advantageous, because it renders the Kubo-transformed velocity CF less affected by errors in the Boltzmann Wigner transform. For simplicity, in the following, we shall consider only a one-dimensional problem. The corresponding multidimensional equations follow straightforwardly by adopting a procedure similar to that taken in the Appendix of ref 37, where the multidimensional FK−LPI Van Hove CF was derived. We will need the one-dimensional version of the Wigner transform in eq 2, expressed in the momentum representation:

$$(\hat{C})_W[q, p] = \int_{-\infty}^{+\infty}\mathrm{d}\xi\, \exp\left(\frac{iq\xi}{\hbar}\right)\left\langle p + \frac{1}{2}\xi\middle|\hat{C}\middle|p - \frac{1}{2}\xi\right\rangle \qquad (16)$$

We first derive eq 1 corresponding to $\langle\hat{A}(0)\hat{B}(s)\rangle = \langle\hat{v}(0)\hat{v}(s)\rangle$, $\hat{v} \equiv \hat{p}/M$, and, afterward, proceed with the Kubo case.

3.1. FK−LPI Form for Normal Velocity CF. From eqs 1 and 4, it follows that we need the quantity $(\hat{\delta}_{FK}(x_c, p_c)\hat{v})_W[q, p]$.

It can be evaluated by substituting $\hat{v}$ times the quasi-density operator of eq 9 into the Wigner transform given by eq 16. The result is

$$(\hat{\delta}_{FK}(x_c, p_c)\hat{v})_W[q, p] = \frac{2}{\alpha}\left(\frac{p}{M} - i\frac{(q - x_c)}{\alpha}\Omega(x_c)\right) \times \exp\left(-\frac{M\Omega(x_c)}{\hbar\alpha}(q - x_c)^2 - \frac{1}{M\Omega(x_c)\alpha\hbar}(p - p_c)^2\right) \quad (17)$$

Only the real part of $\langle v(0)v(s)\rangle$ should be used in eq 13. Henceforth, we arrive at the following FK−LPI expression for the normal velocity CF:

$$\langle v(0)v(t)\rangle_{Real} = \frac{1}{2\pi\hbar}\frac{1}{Z_{FK}}\int\int dx_c\, dp_c \rho_{FK}(x_c, p_c) \int\int dq\, dp \frac{2}{\alpha} v v_t \times \exp\left[-\frac{M\Omega(x_c)}{\hbar\alpha}(q - x_c)^2 - \frac{1}{M\Omega(x_c)\alpha\hbar}(p - p_c)^2\right] \quad (18)$$

where v_t is the velocity of the classically propagated particle at time t.

3.2. FK−LPI Form for Kubo-Transformed Velocity CF. The procedure is almost identical to that adopted in Section 3.1. However, we first need to utilize the identity[21]

$$\int\int dx_c\, dp_c \frac{1}{Z}\rho(x_c, p_c)\hat{\delta}(x_c, p_c)p_c = \left(\frac{1}{\beta\hbar}\right)\frac{1}{Z}\int_0^{\beta\hbar} ds \exp(-(\beta - s)\hat{H})\hat{p} \exp(-s\hat{H}) \quad (19)$$

which is *exact*, provided that the exact centroid density and quasi-density operator are used. Substituting these by their effective frequency counterparts, we obtain

$$\left(\frac{1}{\beta\hbar}\right)\frac{1}{Z}\int_0^{\beta\hbar} ds \exp(-(\beta - s)\hat{H})\hat{p} \exp(-s\hat{H}) \approx \frac{1}{Z_{FK}}\int\int dx_c\, dp_c \rho_{FK}(x_c, p_c)\hat{\delta}_{FK}(x_c, p_c)p_c \quad (20)$$

Multiplying both sides of eq 20 with the Heisenberg operator $\hat{p}(t)$, followed by taking the trace, we obtain

$$\left(\frac{1}{\beta\hbar}\right)\frac{1}{Z}\int_0^{\beta\hbar} ds\, \mathrm{Tr}\{\exp(-(\beta - s)\hat{H})\hat{p} \exp(-s\hat{H})\hat{p}(t)\} \approx \frac{1}{Z_{FK}}\int\int dx_c\, dp_c\, p_c \rho_{FK}(x_c, p_c)\mathrm{Tr}\{\hat{\delta}_{FK}(x_c, p_c)\hat{p}(t)\} \quad (21)$$

Next, we apply the LPI or classical Wigner approximation in eq 3:

$$\mathrm{Tr}\{\hat{\delta}_{FK}(x_c, p_c)\hat{p}(t)\} \approx \frac{1}{(2\pi\hbar)}\int\int dq\, dp\, (\hat{\delta}_{FK}(x_c, p_c))_W[q, p]p_t \quad (22)$$

which, when utilized in eq 21, yields

$$\langle p(0)p(t)\rangle_K \approx \frac{1}{(2\pi\hbar)}\frac{1}{Z_{FK}}\int\int dx_c\, dp_c\, p_c \rho_{FK}(x_c, p_c) \times \int\int dq\, dp\, (\hat{\delta}_{FK}(x_c, p_c))_W[q, p]p_t \quad (23)$$

or

$$\langle v(0)v(t)\rangle_K \approx \left(\frac{1}{2\pi\hbar}\right)\frac{1}{Z_{FK}}\int\int dx_c\, dp_c\, v_c \rho_{FK}(x_c, p_c) \int\int dq\, dp \left(\frac{2}{\alpha}\right) \times \exp\left[-\frac{M\Omega(x_c)}{\hbar\alpha}(q - x_c)^2 - \frac{1}{M\Omega(x_c)\alpha\hbar}(p - p_c)^2\right] v_t \quad (24)$$

Equation 24 constitutes the FK−LPI version of the Kubo-transformed velocity CF.

3.3. Relation between Kubo-Transformed Velocity CF Given by FK−LPI and CMD. We consider the relation between eq 24 and the Kubo CMD velocity CF.[3] To proceed, we notice that, by defining a *dynamical* centroid variable through

$$v_c(t) \equiv \frac{1}{2\pi\hbar}\int\int dq\, dp\, (\hat{\delta}(x_c, p_c))_W[q, p]v_t \approx \frac{1}{2\pi\hbar}\int\int dq\, dp\, (\hat{\delta}_{FK}(x_c, p_c))_W[q, p]v_t = \frac{1}{2\pi\hbar}\int\int dq\, dp \left(\frac{2}{\alpha}\right) \times \exp\left[-\frac{M\Omega(x_c)}{\hbar\alpha}(q - x_c)^2 - \frac{1}{M\Omega(x_c)\alpha\hbar}(p - p_c)^2\right] v_t \quad (25)$$

one has, in fact, derived the FK−LPI analogue of CMD. To see this, we first observe that $v_c(t)$ is indeed identical to $v_c = p_c/M$ when $t = 0$,[60] so that the new *time-dependent* velocity centroid variable collapses to the well-defined old *time-independent* centroid variable. Next, substitute eq 25 into eq 24 to obtain

$$\langle v(0)v(t)\rangle_K \approx \frac{1}{Z_{FK}}\int\int dx_c\, dp_c\, v_c \rho_{FK}(x_c, p_c)v_c(t) \quad (26)$$

which is exactly in a form identical to that of the CMD Kubo-transformed velocity CF.[3] It is not hard to show that eq 26 and the corresponding CMD expression[3] yields the same Taylor series expansion of $\langle v(0)v(t)\rangle_K$ up to second order in the time step, provided the same centroid density $\rho_{FK}(x_c, p_c)$ and quasi-density operator $\hat{\delta}_{FK}(x_c, p_c)$ are used in both expressions. The Kubo-transformed LPI velocity CF is exact to fourth order in the time step, if $\rho_{FK}(x_c, p_c)$ and $\hat{\delta}_{FK}(x_c, p_c)$ were exact, as shown in the Appendix.

3.4. Robustness of Kubo-Transformed Velocity CF toward Errors in Boltzmann Wigner Transform. We now turn to a discussion of the relative quality of the numerical performance of the Kubo-transformed velocity CF in eq 24, as compared to the normal form in eq 18. We consider a Taylor expansion of the two CFs. Let us focus on the first expansion term, i.e., the initial value of the CFs. From eq 18, it is observed that the initial value of the normal velocity CF is dependent on quantum smearing through the factor $(1/M\Omega(x_c)\alpha\hbar)$. If this factor is wrong, the initial value of $\langle v(0)v(t)\rangle$ also will be wrong. From eq 24 or eq 26, it is observed that the initial value of $\langle v(0)v(t)\rangle_K$ equals $\langle v_c(0)v_c(0)\rangle_K$, which is the classical value k_BT/M. This value is the exact value of $\langle v(0)v(0)\rangle_K$ and is obviously independent of the thermal smearing factor $(1/M\Omega(x_c)\alpha\hbar)$. Hence, errors in the Boltzmann Wigner transform degrade the initial value of $\langle v(0)v(t)\rangle$ but not the initial value of $\langle v(0)v(t)\rangle_K$. One may next compare the second terms in the Taylor expansions of the real part of $\langle v(0)v(t)\rangle$ and $\langle v(0)v(t)\rangle_K$, which

are the t^2 terms. From eqs 18 and 24, it follows straightforwardly that the derivatives are

$$\frac{\mathrm{d}^2}{\mathrm{d}t^2}\langle v(0)v(t)\rangle|_{t=0} = -\left(\frac{1}{2\pi\hbar}\right)\frac{1}{Z_{\mathrm{FK}}}\int\int \mathrm{d}x_c\,\mathrm{d}p_c\,\rho_{\mathrm{FK}}(x_c,p_c)\times \int\int \mathrm{d}q\,\mathrm{d}p\frac{2}{\alpha}v^2\frac{1}{M}\frac{\mathrm{d}^2V(q)}{\mathrm{d}q^2}\times \exp\left[-\frac{M\Omega(x_c)}{\hbar\alpha}(q-x_c)^2-\frac{1}{M\Omega(x_c)\alpha\hbar}(p-p_c)^2\right] \quad (27)$$

and

$$\frac{\mathrm{d}^2}{\mathrm{d}t^2}\langle v(0)v(t)\rangle_{\mathrm{K}}|_{t=0} = -\frac{1}{Z_{\mathrm{FK}}}\int\int \mathrm{d}x_c\,\mathrm{d}p_c\,{v_c}^2\rho_{\mathrm{FK}}(x_c,p_c)\times \left\{\sqrt{\frac{M\Omega(x_c)}{\pi\hbar\alpha}}\int \mathrm{d}q\frac{1}{M}\frac{\mathrm{d}^2V(q)}{\mathrm{d}q^2}\exp\left[-\frac{M\Omega(x_c)}{\hbar\alpha}(q-x_c)^2\right]\right\} \quad (28)$$

From these equations, we see that the second moment of the Kubo-transformed CF differs from the classical second moment through only the adoption of a "quantum smeared" Hessian term (the quantity in curly brackets), instead of a classical Hessian evaluated at x_c. No momentum smearing is present. The second moment of the normal velocity CF, on the other hand, contains a smeared term of type $v^2(\mathrm{d}^2V(q)/\mathrm{d}q^2)$, the value of which clearly is dependent both on momentum and position quantum effects. One concludes that the second moment of the Kubo CF is less dependent on quantum effects and, henceforth, less affected by errors in the Boltzmann Wigner transform. One may continue this analysis to higher-order terms in the Taylor series; however, the trend is not hard to see. The coefficient pertaining to the $2n$th time derivative in the Taylor expansion of the normal velocity CF will contain the average of a p^{2n} term, whereas the corresponding coefficient in the Kubo Taylor series will contain only a $p^{2(n-1)}$ term. The lower the moment, the more stable the coefficient value will be against errors in the Wigner transform.

We finally note that the FK−LPI approximation to both the Kubo-transformed and normal velocity CF would be exact to fourth order in the time step, if the FK centroid density and quasi-density operator were exact (see Appendix). This follows because both LPI versions apply the same dynamical approximation: $(\hat{p}(t))_{\mathrm{W}}[q,p] \approx (\hat{p})_{\mathrm{W}}[q_t,p_t]$, which is exact to fourth order in a Taylor expansion in t. Moreover, the (q, p) vectors have the same weight in the two FK−LPI versions, as is apparent from eqs 18 and 24. Hence, there are no obvious reasons why the Kubo-transformed velocity CF should be more accurate *if* the initial conditions were exact. The conclusion then must be the following: if the Kubo-transformed velocity CF performs better, it is *only* because errors in the quantum initial conditions have a smaller effect on it, as compared to the normal velocity CF.

4. FK−LPI Molecular Dynamics Simulation

4.1. Potential. To perform FK−LPI molecular dynamics of para-hydrogen at $T = 17$ and 25 K, we consider 125 H_2 molecules in a cubic simulation box. The interaction between two para-hydrogen molecules is described by the Silvera−Goldman (SG) potential,[47] which treats the molecules as spherical particles. This simplification is permissible because, at low temperature, the molecules are in a single-molecule free rotor state and only the para ($J = 0$) state, not ortho ($J = 1$) state, is populated, because of the large splitting of several hundreds of Kelvin degrees between the ortho/para states:[11]

TABLE 1: Silvera−Goldman Potential Parameters for Para-hydrogen

parameter	value
α	1.713 a.u.
β	1.5671 a.u.
γ	0.00993 a.u.
C_6	12.14 a.u.
C_8	215.2 a.u.
C_9	143.1 a.u.
C_{10}	4813.9 a.u.
r_m	6.501 a.u.

$E = BJ(J+1)$, $B \approx 85.4$ K. The single-molecule rotor wave functions are spherical symmetric for the $J = 0$ (para) state. Thus, the interaction between two molecules is dependent only on the center-of-mass distance, r, through[47]

$$V_{\mathrm{SG}}(r) = \Phi_{\mathrm{rep}}(r) + \Phi_{\mathrm{att}}(r)f_c(r) + \frac{C_9}{r^9}f_c(r) = \exp(\alpha-\beta r-\gamma r^2) - \left(\frac{C_6}{r^6}+\frac{C_8}{r^8}+\frac{C_{10}}{r^{10}}\right)f_c(r) + \frac{C_9}{r^9}f_c(r) \quad (29)$$

The first term in eq 29 represents an exponential SCF repulsion, the second term represents a van der Waals attraction, and the last term represents an effective two-body term incorporating many-body forces.[47] The term $f_c(r)$ turns the attraction off when the molecules approach each other closely:

$$f_c(r) = \begin{cases} \exp\left[-\left(\dfrac{1.28r_m}{r}-1\right)^2\right] & (\text{for } r \le 1.28r_m) \\ 1.0 & (\text{for } r > 1.28r_m) \end{cases} \quad (30)$$

The coefficient values are collected in Table 1. The SG potential has been used in theoretical studies of phase equilibrium[42] and diffusion[3,23,40,41] in liquid para-hydrogen.

4.2. Feynman−Kleinert Wigner Transform. In brief, the construction of quantum initial conditions through the many-dimensional Wigner-transformed Boltzmann operator goes as follows. A Monte Carlo walk in the centroid variables $(\vec{r}_c,\vec{p}_c)$ is performed using the centroid density in eq 5 as a weight function. For a particular $(\vec{r}_c,\vec{p}_c)$ point, the initial conditions for classical dynamics, $(\vec{r},\vec{p})$, are generated via eq 55 from ref 36. To realize this scheme, we utilize the iterative Feynman−Kleinert equations (eqs 50 and 51 from ref 36) to obtain the centroid potential, effective frequencies, and the effective frequency normal modes. To accelerate the implementation of the iterative equations, the H_2-H_2 potential is represented as a sum over Gaussian functions:

$$V_{\mathrm{SG}}(r) = \sum_{i=1}^{n}\gamma_i \exp\left(-\frac{r^2}{2\alpha_i}\right) \quad (31)$$

This makes it possible to evaluate eqs 50 and 54 from ref 36 analytically.[7,36] The present study shows that the use of a sum of four functions indeed allows for an accurate representation. The parameter values are shown in Table 2. Ten iterations of eqs 50 and 51 from ref 36 are utilized to converge the effective frequencies, effective normal modes, and centroid potential. Each iteration involves the diagonalization of the 375×375 dimensional effective frequency matrix of eq 50 from ref 36, which yields the effective frequencies and their normal modes. Once the iterations have converged, the Wigner-transformed Boltzmann operator (eq 55 from ref 36) is constructed and the

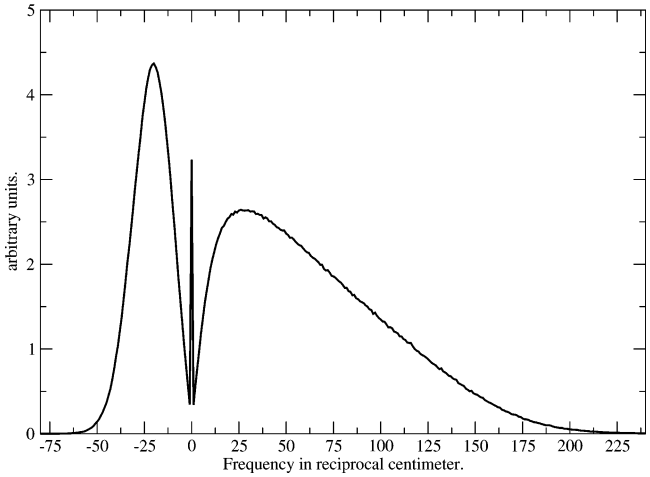

Figure 1. Effective frequency distribution for liquid para-hydrogen at 25 K. Imaginary frequencies are shown according to their absolute values, but on the negative frequency axis.

TABLE 2: Gaussian Potential Form

i	γ_i (a.u.)	α_i (a.u.)
1	0.305797	1.71977
2	−0.0000618932	26.7755
3	0.0461649	2.98876
4	−0.00115682	9.08783

sampling of position and momentum vectors, $(\vec{r},\vec{p})$, is performed via simple Box−Mueller sampling.[38] Ten samplings for each 30th centroid configuration $(\vec{r}_c,\vec{p}_c)$ are performed. A total of 120,000 centroid MC passes is performed for the diffusion/structure problem, using an acceptance ratio of 40%−50%. We should mention that, in the MD implementation of the normal velocity CF, we utilize the multidimensional version of eq 10 (see the Appendix of ref 37).

4.3. Classical Molecular Dynamics Simulation. The quantum mechanical densities at (T = 17 and 25 K) and saturated vapor pressure have been calculated by Scharf and co-workers, using PIMC;[42] these values are 26.9 cm^3/mol and 31.7 cm^3/mol, respectively. For 125 molecules, this is equivalent to a cube of box-length 33.52 bohr (T = 17 K) and 35.41 bohr (T = 25 K). The Gaussian potential (eq 31) is implemented together with the standard minimum image convention and a spherical cutoff at half box-length.[1] The velocity Verlet algorithm, together with a time step of 3 fs, is utilized and the liquid is propagated classically for 11.5 ps. The mass of the para-hydrogen molecules is 3672 a.u. We mention that the actual temperatures used in the simulation deviates from T = 17 and 25 K by an amount equivalent to −1.3%, because of a rounding error in k_B. Accordingly, the actual temperatures are T = 16.8 and 24.7 K. The diffusion coefficients are calculated by integrating eqs 13 and 14 from t = 0 ps to t = 11.5 ps.

5. Results

5.1. Structural Properties. Figures 1 and 2 show the effective frequency distribution for liquid para-hydrogen at 25 and 17 K, respectively. The imaginary portion of the effective frequencies, depicted on the negative axis, is observed to be smaller at 17 K, which is also to be expected, because the density of the liquid is higher at the lower temperature. At 25 and 17 K, the imaginary frequencies extend to −60 and −45 cm^{-1}, respectively. As shown previously,[36] the FK−LPI equations are well-behaved as long as the normal mode imaginary frequencies obey the relation $\hbar|\Omega_i(\vec{r}_c)| \leq \pi k_B T$ (where i = 1, ..., 3N), which is equivalent to requiring that the absolute value of the imaginary frequencies be less than the cut-off values of 55 and 37 cm^{-1} for T = 25 and 17 K, respectively. Hence, a small fraction of frequencies exist that do not allow for a sampling of momenta in the direction of their normal modes. Accordingly, we adopt the rational convention[36] that the momenta sampled along these modes are given by their sampling value reached at the cut-off values, $\pi k_B T/\hbar$; the value is zero.[36]

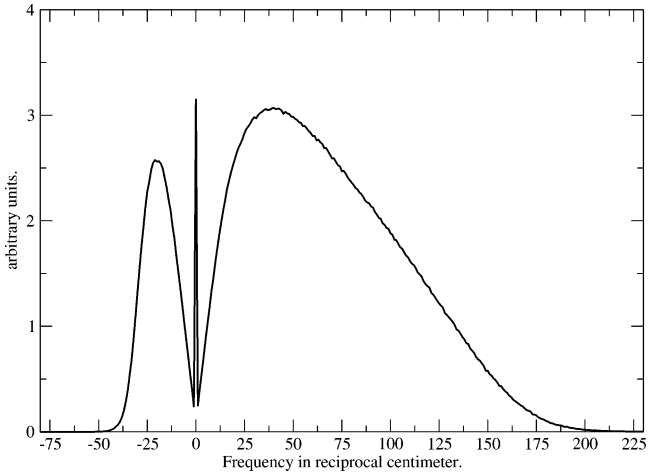

Figure 2. Effective frequency distribution for liquid para-hydrogen at 17 K. Imaginary frequencies are shown according to their absolute values, but on the negative frequency axis.

TABLE 3: Kinetic Energy per Molecule (Divided by k_B) Obtained from Feynman−Kleinert (FK) Boltzmann Wigner Transform, Accurate Path Integral Monte Carlo (PIMC) Calculation, FK−LPI Kubo Velocity CF, and Classical Theory

temperature, T (K)	Kinetic Energy per Molecule (K)[a]			
	FK	PIMC[b]	FK−LPI Kubo	classical
25	63.4 ± 0.4	61.9	61.3 ± 1.2	37.5
17	67.1 ± 0.3	62.0	61.6 ± 0.8	25.5

[a] Divided by k_B. [b] From ref 34.

The kinetic energy per molecule, in units of k_B, is obtained from the initial value of the normal velocity CF function. The calculated FK−LPI values at the two thermodynamic points are shown in Table 3, together with classical values and accurate PIMC values.[34] Also shown are results obtained from the FK−LPI Kubo velocity CF, derived by mapping the Kubo CF onto the normal velocity CF by utilizing a well-known Fourier relation.[57] One observes a very good agreement between FK−LPI and the accurate result at 25 K (agreement within ∼3% is observed), whereas the discrepancy between results from the normal FK-LPI velocity CF and PIMC is almost 10% at 17 K. This clearly shows that the effective frequency theory performs well at 25 K but is not precise enough at 17 K. Interestingly, the FK−LPI Kubo-based kinetic energy is still very good at 17 K. The fact that the accuracy of the effective frequency theory degrades as the temperature is reduced is well-known.[24] However, the critical temperature where failure sets in is, of course, system-dependent, and, to our knowledge, has never been studied previously, for a realistic condensed phase system.

We next turn to the radial distribution function, $g(r)$, for para-hydrogen at the two temperatures. The calculated FK−LPI $g(r)$ function for T = 25 and 17 K is shown is Figures 3 and 4, respectively. The accurate PIMC results of Nakayama and Makri[34] also are shown. Here, we note a very good agreement

TABLE 4: Diffusion Coefficients Obtained by Various Methods[a]

temperature, T (K)	Diffusion Coefficient, D (Å^2/ps^2)								
	ME	CMD	FB−SC	FK−LPI(Kubo)	FK−LPI	MC	ASWPIMD	Cl	Exp
25	1.47[b]	1.54[c]	1.68[e]	1.73	1.94	1.69[f]	2.2[g]	0.5[c]	1.6[h]
17		0.47[d]	0.88[e]	0.83	1.20				0.68[h]

[a] Abbreviation legend is as follows: ME, maximum entropy; CMD, centroid molecular dynamics; FB−SC, forward−backward semiclassical dynamics; FK-LPI, Feynman−Kleinert linearized path integral; MC, mode coupling theory; ASWPIMD, adiabatic separable Wigner path integral molecular dynamics; Cl, classical molecular dynamics; and Exp, experiment. [b] From ref 40. [c] From ref 3. [d] From ref 54. [e] From ref 34. [f] From ref 41. [g] From ref 4. [h] From ref 12.

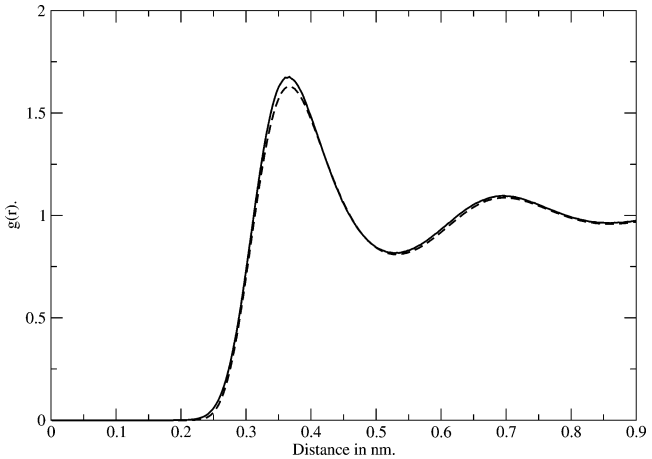

Figure 3. Radial distribution function ($g(r)$) for liquid para-hydrogen at 25 K: (—) FK−LPI and (- - -) PIMC.

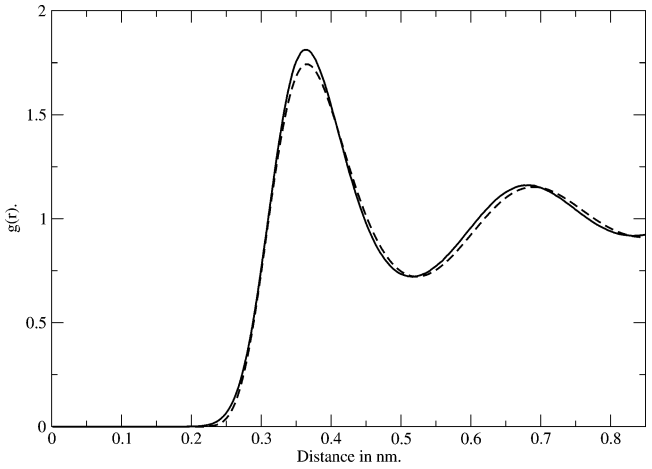

Figure 4. Radial distribution function $g(r)$ for liquid para-hydrogen at 17 K: (—) FK−LPI and (- - -) PIMC.

between FK−LPI and the accurate $g(r)$ functions at both temperatures, but particularly at 25 K.

The aforementioned results seem to indicate that the effective frequency Wigner transform is quite accurate at 25 K but less accurate at 17 K. It is interesting to compare the aforementioned structural predictions of the FK effective frequency theory with the results of Nakayama and Makri,[34] who utilized the so-called single-bead pair-product approximation (PPA)[8] (a many-body action is approximated by the exact action of two interacting atoms) to determine the structure of liquid para-hydrogen at $T = 17$ and 25 K. Comparing Figure 3 with Figure 2 of ref 34, one notices that the PPA-based $g(r)$ function is less accurate than the corresponding $g(r)$ from FK theory. Moreover, the kinetic energies per particle from FK theory and PPA are, more or less, the same: PPA predicts 66.5 K (at 17 K) and 64.0 K (at 25 K), whereas FK theory yields 67.1 K (at 17 K) and 63.4 K (at 25 K). Hence, the overall performance of single-bead PPA and FK effective frequency theory favors the latter.

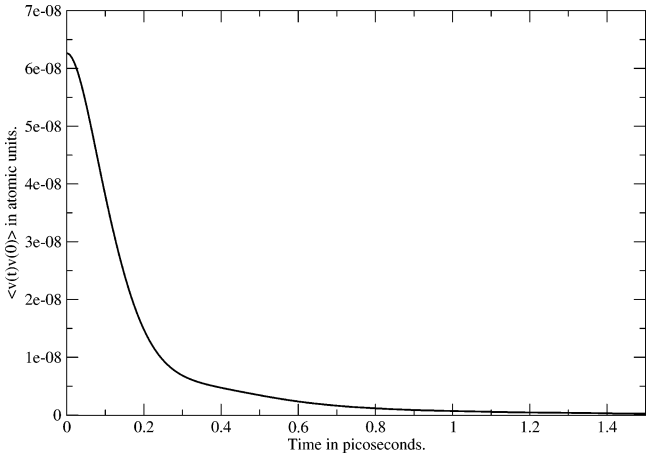

Figure 5. Kubo-transformed velocity CF for liquid para-hydrogen at 25 K.

5.2. Dynamical Results. As already stated, many different theoretical methods have been applied to the para-hydrogen diffusion problem. Among these methods, we find the following: an algorithm based on maximum entropy (ME) analytical continuation of the imaginary time Kubo-transformed velocity CF;[40] centroid molecular dynamics (CMD) approximation to Kubo-transformed velocity CF;[3,31,54] forward−backward semiclassical dynamics (FB−SC);[34] mode-coupling (MC) theory,[41] also targeted at Kubo-transformed velocity CF; and finally adiabatic separable Wigner path integral molecular dynamics (ASWPIMD).[4] Table 4 shows the diffusion coefficients predicted by the various methods, as well as the experimental values[12] for both 25 and 17 K. The values are discussed below.

5.2.1. Velocity Correlation Functions at 25 K. The calculated Kubo-transformed velocity CF based on FK−LPI theory, for $T = 25$ K, is shown in Figure 5. From this figure, we see that the CF decays rapidly until ∼0.3 ps, where a slow decay then takes control. The overall shape of this FK−LPI CF is in good agreement with the Kubo-transformed velocity CF that was reported by Pavese and Voth, who considered the same thermodynamic point, using pseudo-potential CMD.[35] The velocity CF of Pavese and Voth also shows a fast decay until ∼0.3 ps. Both CFs remain positive for all times. From Table 4, we see that the predicted FK−LPI value of 1.73 Aa^2/ps is in very good agreement with both experiment (1.6 Aa^2/ps) and the values obtained by CMD, FB−SC, and mode-coupling theory.

In Figure 6, we present the normal velocity CF at 25 K. It reaches a plateau after 0.25 ps. This feature is in good agreement with the normal velocity CF that is computed, at the same thermodynamic point, via a maximum entropy scheme[40] and CMD,[3] both of which also possess a plateau near $t = 0.25$ ps. On the other hand, the same CF, when calculated by mode-coupling theory,[41] is predicted to reach an approximate plateau first after 0.55 ps. The same velocity CF, computed via forward−backward semiclassical dynamics,[34] has yet another

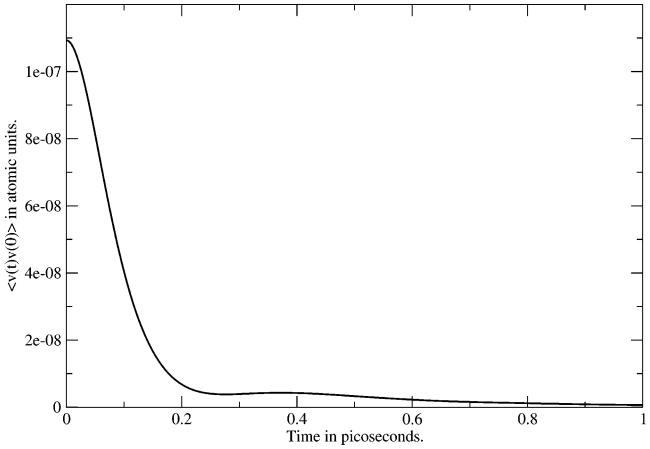

Figure 6. Velocity CF for liquid para-hydrogen at 25 K.

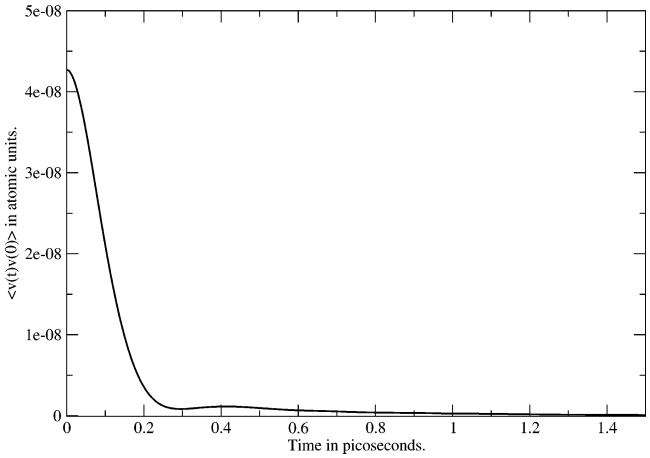

Figure 7. Kubo-transformed velocity CF for liquid para-hydrogen at 17 K.

behavior with essentially a plateau-free shape. The FK−LPI value of the diffusion coefficient that follows from the data in Figure 6 (1.94 Aa^2/ps) is still in good agreement with experiment, especially when compared to the more-involved ASW-PIMD method.

5.2.2. Velocity Correlation Functions at 17 K. In Figure 7, we represent the Kubo-transformed velocity CF based on FK−LPI theory for $T = 17$ K. It is characterized by a fast decay until ∼0.25 ps, where it essentially has attained its long-time value of zero. We can compare the FK−LPI Kubo-transformed velocity CF with that of Yonetani and Kinugawa,[54] who calculated the same CF at approximately the same thermodynamic point using CMD. Although the two Kubo CFs share the time $t = 0.25$ ps as a turning point, the two CFs disagree, in that the Kubo velocity CF of Yonetani and Kinugawa exhibits a pronounced minimum with negative values, whereas the FK−LPI CF does not become negative. The FK−LPI diffusion coefficient of 0.83 Aa^2/ps is in reasonable agreement with the experimental value of 0.68 Aa^2/ps.

Figure 8 shows the normal velocity CF, as calculated by FK−LPI. The FK−LPI CF now has a small negative component. Again, the minimum is attained at $t = 0.25$ ps. At this thermodynamic point, we do not have any figures of normal velocity CFs from literature reports. From Table 4, we note the limits on the performance of FK−LPI when applied to the determination of the normal velocity CF, yielding a value of 1.20 Aa^2/ps, which, as we have argued, is most likely caused by errors in the Boltzmann Wigner transform.

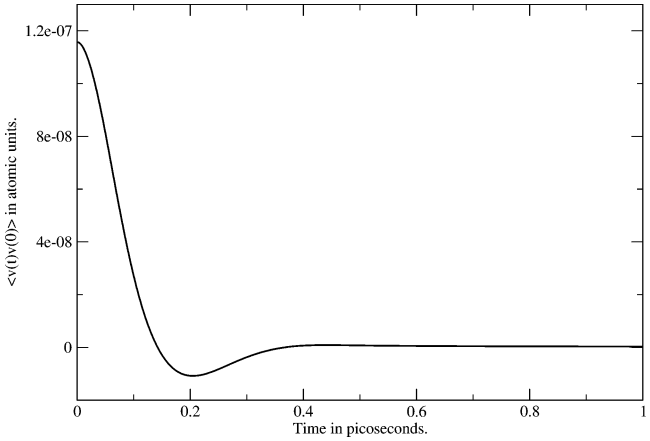

Figure 8. Velocity CF for liquid para-hydrogen at 17 K.

6. Summary and Discussion

6.1. Summary. The Feynman−Kleinert (FK) effective frequency representation of path integrals has been used to generate the Wigner-transformed Boltzmann operator for liquid para-hydrogen at almost zero pressure and temperatures of $T = 17$ and 25 K. The center-of-mass radial distribution function and the kinetic energy of the liquid have been calculated at the two thermodynamic points. Also, the molecular center-of-mass diffusion coefficients have been calculated at both temperatures. The radial distribution functions were determined to be in excellent agreement with accurate path integral Monte Carlo (PIMC) calculations, whereas the kinetic energy of the liquid was less accurately described at $T = 17$ K. It was concluded that the effective frequency theory is deteriorating at $T = 17$ K. However, the structural properties derived from effective frequency theory were still observed to be in better agreement with accurate PIMC results, when compared to similar results obtained by a pair-product approximation.[8,34]

The ordinary velocity CF, as well as the Kubo-transformed velocity CF, have been calculated, at both thermodynamic points, using the Feynman−Kleinert linearized path integral (FK−LPI) methodology. The diffusion coefficients based on the Kubo-transformed velocity CF were in very good agreement with the experiment, at both temperatures, whereas the diffusion coefficient values derived from the ordinary velocity CF only agreed well with the experiment at 25 K. The kinetic energy of the liquid, predicted by the Kubo velocity CF, was in excellent agreement with accurate results at both temperatures. An analysis of the Taylor series expansion of the various velocity CFs showed, in agreement with the aforementioned findings, that the Kubo-transformed velocity CF is more robust against errors in the Boltzmann Wigner transform. It was moreover demonstrated that both the FK−LPI approximation to the Kubo-transformed velocity CF and the normal velocity CF are exact to the fourth order in the time step, provided a hypothetical exact Boltzmann Wigner distribution was used. These last two observations then lead to the conjecture that the reason for the poorer performance of the ordinary velocity CF is due to errors in the initial Wigner distribution function.

6.2. Discussion. The errors in the diffusion coefficients obtained by FK−LPI are produced by either errors in the Wigner distribution of the Boltzmann operator or errors in the propagation of the Wigner-transformed momentum Heisenberg operator (see eq 3). The structural results suggest that the Wigner transform, although not being exact, is close to being accurate at 25 K. Hence, any error in the diffusion coefficient should then, to a good approximation, be caused by errors in the

dynamics, i.e., in the LPI approximation. This holds true in particular for the diffusion coefficient derived from the Kubo velocity CF, which was shown to be the most-stable diffusion coefficient against Wigner transform errors. At 25 K, we observe a very good agreement between the experimental result and the Kubo diffusion coefficient. This then indicates that the underlying classical Wigner or LPI approximation of eq 3 is working well at 25 K. Unfortunately, the Feynman and Kleinert (FK) Wigner transform is not as accurate at 17 K and, therefore, any discrepancy between the experimental diffusion coefficient and the FK−LPI counterpart cannot be explained by a fault alone in the dynamical LPI or classical Wigner approximation. Therefore, although the FK−LPI Kubo diffusion coefficient is in relatively good agreement with the experiment, also at 17 K, one cannot rule out the possibility that an even better Boltzmann Wigner transform would produce a better LPI Kubo diffusion coefficient value. Therefore, we think it is fair to say that the FK−LPI method has been shown to predict diffusion coefficients for para-hydrogen at $T = 17$ and 25 K successfully, when based on the Kubo-transformed velocity CF. This conclusion has the implication that, at these temperatures, *classical* dynamics is adequate for propagating the Wigner-transformed momentum Heisenberg operator, when studying diffusion in para-hydrogen.

We next consider the future applications of the FK−LPI method, as well as discuss various possible ways of improving the efficiency of the effective frequency implementation.

The FK−LPI method clearly represents an approximate method for doing quantum dynamics. As the present work has shown, the structure of liquid para-hydrogen is described faithfully at 25 K but less accurately at 17 K; the FK kinetic energy at 17 K is wrong by almost 10%. This means that the FK effective frequency theory, in its present form, cannot be used to study, e.g., liquid density fluctuations in nonsuperfluid He(4) at 4 K,[33] because the FK Boltzmann Wigner transform cannot be expected to be accurate at such low temperatures. In this connection, we recognize a simple way of improving on the accuracy of the FK Boltzmann Wigner transform. One utilizes a Boltzmann operator splitting ($\exp(-\beta\hat{H}) = \exp(-\beta\hat{H}/2) \times \exp(-\beta\hat{H}/2)$) and, afterward, applies eq 4 to each operator. We still have an analytical Boltzmann Wigner transform; however, one now needs to simultaneously consider *two* sets of centroid coordinates, effective frequencies, and normal modes in the FK−LPI implementation. Clearly, the workload is doubled but the lowest temperature at which the FK Wigner distribution is accurate is now halved, as compared to the normal FK implementation in this paper. Hence, this approach could be used to generate a more-accurate Wigner distribution function for para-hydrogen at 17 K.

Limiting the discussion to the original FK−LPI method, without splitting, one may ask what type of liquids allow for an accurate Wigner transform based on FK effective frequency theory? What about room-temperature systems such as, e.g., water? We conjecture that the liquid water Boltzmann Wigner transform can be obtained accurately from FK theory. Based on the para-hydrogen results for 25 K, we see that the FK theory accurately calculates the Boltzmann Wigner transform for a liquid whose characteristic frequencies are 5−6 times larger than k_BT ($k_BT \approx 20$ cm^{-1}, at 25 K); see Figure 1. Room-temperature water is, more or less, just as quantum mechanical: Water has librational modes with frequency values up to 1000 cm^{-1},[49] which should be compared to $k_BT \approx 220$ cm^{-1}. Of course, the intramolecular OH stretch modes have a much larger $\hbar\omega/(k_BT)$ ratio; however, to the extent that they are harmonic, the FK effective frequency theory will provide a satisfactory description, because FK theory is correct for harmonic systems.

In the present study, we have determined the effective frequencies, their normal modes, and the centroid potential via the iterative approach of Feynman and Kleinert (FK).[24] This involves diagonalization of $3N \times 3N$ dimensional matrixes, with $3N$ being the number of degrees of freedom. This approach becomes inefficient for systems that already contain ∼200 atoms. Fortunately, because the FK effective frequency theory is variational,[13,24] one may instead utilize an extended Lagrangian procedure that is based on molecular dynamics.[7] Such an implementation could, in principle, extend the FK machinery to much larger systems. In connection, we conclude that this is an advantage of the FK Boltzmann Wigner transform approach, compared to other Wigner transform schemes that are based on diagonalization, but are nonvariational (see, e.g., ref 44).

The applicability of the present method in its current form has some limitations associated with computational and physical elements. The computational cost is dominated by the diagonalization of a $3N \times 3N$ matrix so that there is a nonlinear dependence on system size. Furthermore, as the system becomes more quantum mechanical, true dynamical effects will enter. It is not simple to predict when these will become important for a given system, because one expects condensed-phase systems to become more harmonic at low temperature, and the present formulation is exact for harmonic systems. We believe that the present results obtained with the FK effective frequency theory justifies additional efforts of implementation—the theory is very general and the present study, and a previous one,[37] have shown it to be surprisingly accurate in predicting structures and kinetic energies in not-too-extreme quantum systems.

Acknowledgment. J.A.P. and G.N. gratefully acknowledge support from both the Danish Natural Science Research Council and the Swedish Research Council. P.J.R. gratefully acknowledges support by the National Science Foundation (CHE-0134775) and the Robert A. Welch Foundation. J.A.P. thanks Akira Nakayama and Nancy Makri for kindly providing the accurate para-hydrogen radial distribution functions.

Appendix

Here, we show that the LPI approximation $(\hat{p}(t))_W[q, p] \approx (\hat{p})_W[q_t, p_t]$ is exact, up to fourth order in a Taylor expansion in t. The simplest way to accomplish this would be to calculate $d^4\hat{p}(t)/dt^4|_{t=0} = ((i/\hbar))^4[\hat{H},[\hat{H},[\hat{H},[\hat{H}, \hat{p}]]]]$, compute its Wigner transform, and finally compare that value with the corresponding classical result. However, this fourth-order commutator is rather tedious to evaluate, and we shall, instead, use the Wigner−Liouville equation, which dictates the time evolution of a general Wigner-transformed Heisenberg operator, $(\hat{O}(t))_W[q, p]$:[55]

$$\frac{\partial(\hat{O}(t))_W[q, p]}{\partial t} = \frac{\partial H(q, p)}{\partial p}\frac{\partial(\hat{O}(t))_W[q, p]}{\partial q} - \frac{\partial H(q, p)}{\partial q}\frac{\partial(\hat{O}(t))_W[q, p]}{\partial p} + \int_{-\infty}^{+\infty} dp' w(p - p', q)(\hat{O}(t))_W[q, p'] \quad (32)$$

where

$$w(p - p', q) = \frac{i}{2\pi\hbar^2}\int_{-\infty}^{+\infty} d\xi \exp[i/\hbar\xi(p - p')] \times \left\{V\left(q - \frac{\xi}{2}\right) - V\left(q + \frac{\xi}{2}\right) + \xi V'(q)\right\} \quad (33)$$

H is the classical Hamiltonian. The last term defined (w, the "quantum term"), is responsible for all dynamical nonclassical effects and vanishes for harmonic potentials. By differentiating eq 32 three times, with respect to t, we obtain

$$\frac{\partial(\hat{O}^{(3)}(t))_W[q,p]}{\partial t} = \frac{\partial H(q,p)}{\partial p}\frac{\partial(\hat{O}^{(3)}(t))_W[q,p]}{\partial q} - \frac{\partial H(q,p)}{\partial q}\frac{\partial(\hat{O}^{(3)}(t))_W[q,p]}{\partial p} + \int_{-\infty}^{+\infty} dp' w(p-p',q)(\hat{O}^{(3)}(t))_W[q,p'] \quad (34)$$

where $(\hat{O}^{(n)}(t))_W[q,p] \equiv ((d^n/dt^n)\hat{O}(t))_W[q,p]$. From the aforementioned discussion, it follows that we must use $(\hat{O}(t))_W[q,p] = (\hat{p}(t))_W[q,p]$, evaluate eq 34 for $t = 0$, and show that the quantum term vanishes. If this holds true, then we have

$$\left.\frac{\partial(\hat{p}^{(3)}(t))_W[q,p]}{\partial t}\right|_{t=0} = \frac{\partial H(q,p)}{\partial p}\frac{\partial(\hat{p}^{(3)}(t=0))_W[q,p]}{\partial q} - \frac{\partial H(q,p)}{\partial q}\frac{\partial(\hat{p}^{(3)}(t=0))_W[q,p]}{\partial p} \quad (35)$$

Furthermore, using eq 16,

$$(\hat{p}^{(3)}(t=0))_W[q,p] = \left[\frac{-1}{4M^2}\{\hat{p}^2V^{(3)} + 2\hat{p}V^{(3)}\hat{p} + V^{(3)}\hat{p}^2\} + \frac{V^{(2)}V^{(1)}}{M}\right]_W[q,p] = \frac{-p^2}{M^2}V^{(3)}(q) + \frac{V^{(1)}(q)V^{(2)}(q)}{M} \quad (36)$$

which is just the classical result, Thus, it follows from eq 35 that the derivative $(\hat{p}^{(4)}(t))_W[q,p]|_{t=0}$ is equal to its classical counterpart, as given by the FK−LPI method, and we are finished. To show that the quantum term vanishes, we make use of the identity[52]

$$\int_{-\infty}^{+\infty} dp' w(p-p',q)(\hat{O}^{(3)}(t=0))_W[q,p'] = \sum_{n=1}^{\infty}\frac{\partial^{2n+1}(\hat{O}^{(3)}(t=0))_W[q,p]}{\partial p^{2n+1}}\left(\frac{\hbar}{2i}\right)^{2n}\frac{V^{(2n+1)}(q)}{(2n+1)!} \quad (37)$$

which can be obtained by Taylor-expanding $(\hat{O}^{(3)}(t=0))_W[q,p']$ around p and doing some integration by parts. However, all terms in eq 37 vanish, because $(\hat{O}^{(3)}(t=0))_W[q,p] = (\hat{p}^{(3)}(t=0))_W[q,p]$ is, at most, quadratic in p (see eq 36).

References and Notes

(1) Allen, M. P.; Tildesley, D. J. *Computer Simulations of Liquids*; Oxford University Press: Oxford, U.K., 1987.
(2) Caldeira, A. O.; Leggett, A. J. *Physica A* **1983**, *121A*, 587−616.
(3) Calhoun, A.; Pavese, M.; Voth, G. A. *Chem. Phys. Lett.* **1999**, *262*, 415.
(4) Cao, J.; Martyna, G. J. *J. Chem. Phys.* **1996**, *104*, 2028−2035.
(5) Cao, J.; Voth, G. A. *J. Chem. Phys.* **1994**, *100*, 5106−5117.
(6) Cao, J.; Voth, G. A. *J. Chem. Phys.* **1994**, *101*, 6184−6192.
(7) Cao, J.; Voth, G. A. *J. Chem. Phys.* **1994**, *101*, 6168−6183.
(8) Ceperley, D. M. *Rev. Mod. Phys.* **1995**, *67*, 279−355.
(9) Cuccoli, A.; Giachetti, R.; Tognetti, V.; Vaia, R.; Verrucchi, P. *J. Phys.: Condens. Matter* **1995**, *7*, 7891−7938.
(10) Cuccoli, A.; Tognetti, V.; Verrucchi, P.; Vaia, R. *Phys. Rev. A* **1992**, *45*, 8418−8429.
(11) Driessen, A.; Silvera, I. F. *Phys. Rev. B* **1987**, *35*, 6649−6658.
(12) Esel'son, B. N.; Blagoi, Y. P.; Grigor'ev, V. V.; Manzhelii, V. G.; Mikhailenko, S. A.; Neklyudov, N. P. *Properties of Liquid and Solid Hydrogen*; Israel Program for Scientific Translations: Jerusalem, 1971.
(13) Feynman, R. P.; Kleinert, H. *Phys. Rev. A* **1986**, *34*, 5080−5084.
(14) Gell-Mann, M.; Hartle, J. B. *Phys. Rev. D* **1993**, *47*, 3345.
(15) Giachetti, R.; Tognetti, V. *Phys. Rev. Lett.* **1985**, *55*, 912−915.
(16) Giachetti, R.; Tognetti, V. *Phys. Rev. B* **1986**, *33*, 7647−7658.
(17) Giulini, D.; Joos, E.; Kiefer, C.; Kupsch, J.; Stamatescu, I.-O.; Zeh, H. D. *Decoherence and the Appearance of a Classical World in Quantum Theory*; Springer−Verlag: Berlin, 1996.
(18) Heller, E. J. *J. Chem. Phys.* **1976**, *65*, 1289.
(19) Hernandez, R.; Voth, G. A. *Chem. Phys.* **1998**, *223*, 243−255.
(20) Jang, S.; Pak, Y.; Voth, G. A. *J. Phys. Chem. A* **1999**, *103*, 10289−10293.
(21) Jang, S.; Voth, G. A. *J. Chem. Phys.* **1999**, *111*, 2357.
(22) Jang, S.; Voth, G. A. *J. Chem. Phys.* **1999**, *111*, 2371−2384.
(23) Kinugawa, K. *Chem. Phys. Lett.* **1998**, *292*, 454−460.
(24) Kleinert, H. *Path Integrals in Quantum Mechanics, Statistics and Polymer Physics*; World Scientific: Singapore, 1995.
(25) Krilov, G.; Berne, B. J. *J. Chem. Phys.* **1999**, *111*, 9147−9156.
(26) Krilov, G.; Sim, E. Berne, B. J. *J. Chem. Phys.* **2001**, *114*, 1075.
(27) Krilov, G.; Sim, E. Berne, B. J. *Chem. Phys.* **2001**, *268*, 21−34.
(28) Kubo, R.; Toda, M.; Hashitsume, N. *Statistical Physics II*; Springer−Verlag: Berlin, 1985.
(29) Liao, J.-L.; Pollak, E. *J. Chem. Phys.* **1999**, *111*, 7244−7254.
(30) Liao, J.-L.; Pollak, E. *J. Chem. Phys.* **2001**, *116*, 2718−2727.
(31) Martyna, G. J.; Hughes, A.; Tuckerman, M. E. *J. Chem. Phys.* **1999**, *110*, 3275−3290.
(32) Miller, W. H. *J. Phys. Chem. A* **2001**, *105*, 2942−2955.
(33) Miura, S.; Okazaki, S.; Kinugawa, K. *J. Chem. Phys.* **1999**, *110*, 4523−4532.
(34) Nakayama, A.; Makri, N. *J. Chem. Phys.* **2003**, *119*, 8592−8605.
(35) Pavese, M.; Voth, G. A. *Chem. Phys. Lett.* **1996**, *249*, 231−236.
(36) Poulsen, J. Aa.; Nyman, G.; Rossky, P. J. *J. Chem. Phys.* **2003**, *119*, 12179−12193.
(37) Poulsen, J. Aa.; Nyman, G.; Rossky, P. J. *J. Phys. Chem. A* **2004**, *108*, 8743−8751.
(38) Press, W. H.; Teukolsky, S. A.; Vetterling, W. T.; Flannery, B. P. *Numerical Recipes*, Second Edition; Cambridge University Press: Cambridge, U.K., 1992.
(39) Rabani, E.; Krilov, G.; Berne, B. J. *J. Chem. Phys.* **2000**, *112*, 2605.
(40) Rabani, E.; Reichman, D. R.; Krilov, G.; Berne, B. J. *Proc. Natl. Acad. Sci.* **2002**, *99*, 1129−1133.
(41) Reichman, D. R.; Rabani, E. *J. Chem. Phys.* **2002**, *116*, 6279−6285.
(42) Scharf, D. J.; Martyna, G. J.; Klein, M. L. *Low Temp. Phys.* **1993**, *19*, 364.
(43) Shao, J.; Liao, J.-L.; Pollak, E. *J. Chem. Phys.* **1998**, *108*, 9711.
(44) Shi, Q.; Geva, E. *J. Phys. Chem. A* **2003**, *107*, 9059−9069.
(45) Shi, Q.; Geva, E. *J. Phys. Chem. A* **2003**, *107*, 9070−9078.
(46) Shi, Q.; Geva, E. *J. Chem. Phys.* **2003**, *118*, 8173.
(47) Silvera, I. F.; Goldman, V. V. *J. Chem. Phys.* **1978**, *69*, 4209.
(48) Sim, E.; Krilov, G.; Berne, B. J. *J. Phys. Chem. A* **2001**, *105*, 2824−2833.
(49) Stratt, R. M. *Acc. Chem. Res.* **1995**, *28*, 201−207.
(50) Thoss, M.; Wang, H.; Miller, W. H. *J. Chem. Phys.* **2001**, *114*, 9220−9235.
(51) Wang, H.; Sun, X.; Miller, W. H. *J. Chem. Phys.* **1998**, *108*, 9726−9736.
(52) Wigner, E. *Phys. Rev.* **1932**, *40*, 749−759.
(53) Wright, N. J.; Makri, N. *J. Chem. Phys.* **2003**, *119*, 1634−1641.
(54) Yonetani, Y.; Kinugawa, K. *J. Chem. Phys.* **2003**, *119*, 9651−9660.
(55) Zhang, S.; Pollak, E. *J. Chem. Phys.* **2003**, *118*, 4357−4364.
(56) Zwanzig, R. *Annu. Rev. Phys. Chem.* **1965**, *16*, 67−102.
(57) Zwanzig, R. *Nonequilibrium Statistical Mechanics*; Oxford University Press: New York, 2001.
(58) We note that a Boltzmann Wigner transform based on effective frequency theory has previously been considered in ref 10. We thank Ruggero Vaia for bringing this to our attention. However, this paper does not use the quasi-density operator formalism.
(59) Strictly speaking, it is the mean square fluctuation of paths using a PI restricted to paths having a common centroid x_c (from ref 24): $a^2(x_c) \equiv (1/Z_{xc})\int \mathcal{D}x(\tau)(x(\tau) - x_c)^2\delta(\bar{x} - x_c)\exp[(-S(x(\tau))_1/\hbar]$, where S_1 is the Feynman−Kleinert trial action.
(60) This also holds true if the exact quasi-density operator (first line of eq 25) is used.